SIAM J. NUMER. ANAL.
Vol. 60, No. 5, pp. 2435–2447

A MONOTONE, SECOND ORDER ACCURATE SCHEME FOR CURVATURE MOTION*

SELIM ESEDOḠLU† AND JIAJIA GUO‡

Abstract. We present a second order accurate in time numerical scheme for curve shortening flow in the plane that is unconditionally monotone. It is a variant of threshold dynamics, a class of algorithms in the spirit of the level set method that represent interfaces implicitly. The novelty is monotonicity: it is possible to preserve the comparison principle of the exact evolution while achieving second order in time consistency. As a consequence of monotonicity, convergence to the viscosity solution of curve shortening is ensured by existing theory.

Key words. curvature motion, high order scheme, monotone scheme

MSC codes. 65M06, 65M12

DOI. 10.1137/21M1466050

1. Introduction.

In this short note, we report a second order accurate threshold dynamics algorithm for simulating curvature motion (curve shortening) in the plane that is *monotone*: It respects the comparison principle of the exact evolution. Existing theory [2, 13] then immediately implies that the approximate evolution generated by the scheme converges to the viscosity solution of mean curvature motion under appropriate conditions.

The finding is surprising, as previous studies, e.g., [20, 11, 25], that explored the idea of designing high order accurate versions of threshold dynamics speculated that monotonicity may need to be sacrificed. This note shows that, at least in two dimensions, this need not be so. To the best of our knowledge, the algorithm presented is the only one of its kind (level-set style numerical algorithm capable of handling topological changes implicitly) that is rigorously shown to be unconditionally monotone, and consistent to second order, and thereby convergent. All the advantages of the original scheme are retained, as the version proposed here differs only in its choice of convolution kernel, replacing the standard choice of Gaussian with a carefully chosen linear combination of Gaussians. Hence, at least in two dimensions, there is a very special choice of a convolution kernel.

2. Previous work.

There are several relevant contributions to high order in time versions of threshold dynamics in existing literature. The first contribution is from the Ph.D. thesis of Ruuth [20]. There, a second order accurate, multistep scheme inspired by Richardson extrapolation is proposed that is numerically demonstrated to achieve second order accuracy in time in two and three dimensional examples, at least while the evolving interface remains smooth. However, the stability of that scheme (whether by maximum principles or energy methods) appears hard to study, and there are no results to that effect (or even a careful consistency calculation) available.

*Received by the editors December 22, 2021; accepted for publication (in revised form) May 5, 2022; published electronically September 12, 2022.
https://doi.org/10.1137/21M1466050
Funding: The work of the first author was supported by the National Science Foundation (NSF) grant DMS-2012015. The work of the second author was supported by the NSF grant DMS-1813003.
†Department of Mathematics, University of Michigan, Ann Arbor, MI 48109 USA (esedoglu@umich.edu).
‡Corresponding author. Department of Mathematics, University of Michigan, Ann Arbor, MI 48109 USA (jiajiag@umich.edu).

The topic of high order accurate schemes for curvature motion also comes up naturally as a byproduct in studies focused on adapting threshold dynamics to high order geometric motions such as Willmore flow [12, 8], where the idea of using linear combinations of Gaussians as the convolution kernel to cancel out undesirable terms in consistency calculations plays the same prominent role. In [11], designing a second order accurate in time version of threshold dynamics for curvature motion in the plane by a judicious choice of convolution kernel is floated, but the whole approach is based on the incorrect assumption that the curvature of the exact solution can be taken to remain constant during a single time step: The resulting scheme propagates the interface with normal speed given by a second order accurate estimate of the curvature of the exact solution at the end of the time step; this is different from and not sufficient for matching the location of the exact interface at the end of the time step up to a third order local truncation error. Consequently, the proposed scheme is still only first order accurate. Moreover, it is stated that the resulting kernel would not be positive everywhere, and thus the proposed scheme would violate monotonicity.

More recently, second order versions of threshold dynamics were proposed in [25]. One is multistep, similar to that of Ruuth in [20], and therefore not likely to be monotone. However, unlike in [20], it comes with a careful consistency calculation, which verifies second order consistency (in addition to numerical evidence) in two and three dimensions. The other proposed scheme of [25] is multistage, and therefore also unlikely to be monotone. It is, however, second order consistent in two dimensions, and, most notably, satisfies an unconditional energy stability property in any dimension: it dissipates the Lyapunov functional for threshold dynamics discovered in [7]. In the broader context of level-set type methods that represent interfaces implicitly, the early contribution [24] proposes second order, energy (total variation) diminishing schemes for the level set formulation of mean curvature motion, but reports difficulties with (slow or lack of convergence of iterative solvers on) the nonlinear algebraic systems that need to be solved at every time step.

It is also worth recalling that using different (namely, in this case, nonradially symmetric) kernels in threshold dynamics comes up in its extensions to anisotropic curvature flows [22, 3, 5, 6]. In particular, barrier type theorems [5, 6] show that any threshold dynamics scheme that is at all consistent (never mind second order) with certain anisotropic curvature flows in three dimensions cannot possibly be monotone.

3. The standard algorithm.

Recall that the threshold dynamics algorithm of Merriman, Bence, and Osher [19, 18] generates a discrete in time approximation to the motion by mean curvature of an interface $\partial\Sigma^0$ given as the boundary of an initial set $\Sigma^0 \subset \mathbb{R}^d$ by alternating the two steps of convolution and thresholding:

Algorithm:(MBO'92). Given a time step size $t > 0$, alternate the following steps:

1. Convolution:

$$\psi^k = K_t * \mathbf{1}_{\Sigma^k}. \tag{3.1}$$

2. Thresholding:

$$\Sigma^{k+1} = \left\{ x \,:\, \psi^k(x) \geq \lambda \right\}. \tag{3.2}$$

In (3.1), K_t is defined as

$$K_t(x) = \frac{1}{t^{\frac{d}{2}}} K\left(\frac{x}{\sqrt{t}}\right)$$

for a smooth convolution kernel $K : \mathbb{R}^d \to \mathbb{R}$ of total mass $2\lambda > 0$ and sufficiently rapid decay at $|x| \to \infty$. The kernel K was chosen in [19] originally to be the Gaussian:

$$G(x) = \frac{1}{(4\pi)^{\frac{d}{2}}} \exp\left(-\frac{|x|^2}{4}\right), \tag{3.3}$$

but choosing it something else was also raised as a possibility in the same work. With choice (3.3), convergence of scheme (3.1), (3.2) had been established in a number of previous studies, including [9, 1, 13, 23]. There are even convergence results [15, 16] in the multiphase setting.

In this note, we restrict our attention to radially symmetric convolution kernels of the form

$$K(x) = \sum_{j=1}^{N} c_j G_{\alpha_j}(x)$$

and ask whether the coefficients α_j and c_j can be chosen so that

1. $K(x) \geq 0$, and
2. scheme (3.1), (3.2) is second order consistent.

We are surprised to find out that the answer is yes when $d = 2$. Recall that $K(x) \geq 0$ implies unconditional monotonicity of the scheme

$$\Omega^0 \subset \Sigma^0 \Longrightarrow \Omega^k \subset \Sigma^k \quad \text{for all } k = 1, 2, 3, \ldots$$

regardless of the time step size $k > 0$. Preserving this fundamental qualitative feature of the exact evolution is tremendously helpful in establishing stability and convergence of numerical schemes.

4. A special kernel in dimension $d = 2$.

In this section, we carefully exhibit a positive convolution kernel that endows scheme (3.1), (3.2) with second order consistency and, thanks to positivity, monotonicity. Assume that the initial interface is given as the graph of a smooth function $g : \mathbb{R} \to \mathbb{R}$ with $g(0) = 0$ and $g'(0) = 0$, and the initial set is $\Sigma^0 = \{(x, y) : y \geq g(x)\}$. The exact solution $y = \phi(x, t)$ of curvature motion solves the PDE

$$\begin{cases} \phi_t = \dfrac{\phi_{xx}}{1 + \phi_x^2}, \\ \phi(x, 0) = g(x). \end{cases} \tag{4.1}$$

Taylor expanding $\phi(0, t)$ in t at $t = 0$ and converting all time derivatives to spatial ones via the equation, one gets

$$\phi(0, t) = t\, g''(0) + t^2 \left(\frac{1}{2} g^{(\text{iv})}(0) - \left(g''(0)\right)^3(0)\right) + O(t^3) \tag{4.2}$$

as $t \to 0^+$, where $g^{(\text{iv})}$ is the fourth derivative of the function $g(x)$. We will demand that one step of the threshold dynamics scheme gives an interface that crosses the y-axis at $\phi(0, t)$ up to $O(t^3)$ terms.

Taylor expansion for the interface after one step of threshold dynamics using a Gaussian kernel had been obtained in multiple previous studies, e.g., [12, 17, 20, 21].

In particular, formula (4.28) in [20] gives the following expression for the convolution restricted to the y-axis (the initial normal direction):

$$
\begin{aligned}
G_t * \mathbf{1}_\Sigma(0,y) =& \frac{1}{2} - \frac{1}{2\sqrt{\pi}}\frac{y}{\sqrt{t}} + \frac{1}{24\sqrt{\pi}}\frac{y^3}{t^{3/2}} \\
&+ \frac{g''(0)}{2\sqrt{\pi}}\sqrt{t} - \frac{g''(0)}{8\sqrt{\pi}}\frac{y^2}{\sqrt{t}} \\
&+ \frac{g^{(\mathrm{iv})}(0)}{4\sqrt{\pi}}t^{3/2} + \frac{3\big(g''(0)\big)^2}{8\sqrt{\pi}}\sqrt{t}y \\
&- \frac{5\big(g''(0)\big)^3}{8\sqrt{\pi}}t^{3/2} + O(t^{5/2}).
\end{aligned} \tag{4.3}
$$

The first step in those calculations is to expand the convolution step (3.1) of the algorithm along the y-axis, which is, of course, linear in the kernel K. Define

$$\theta(p) = \sum_{j=1}^{N} \alpha_j^{\frac{p}{2}} c_j. \tag{4.4}$$

Using (4.3), we get

$$
\begin{aligned}
K_t * \mathbf{1}_\Sigma(0,y) =& \frac{1}{2}\theta(0) - \frac{1}{2\sqrt{\pi}}\frac{y}{\sqrt{t}}\theta(-1) + \frac{1}{24\sqrt{\pi}}\frac{y^3}{t^{3/2}}\theta(-3) \\
&+ \frac{g''(0)}{2\sqrt{\pi}}\sqrt{t}\theta(1) - \frac{g''(0)}{8\sqrt{\pi}}\frac{y^2}{\sqrt{t}}\theta(-1) \\
&+ \frac{g^{(\mathrm{iv})}(0)}{4\sqrt{\pi}}t^{3/2}\theta(3) + \frac{3\big(g''(0)\big)^2}{8\sqrt{\pi}}\sqrt{t}y\theta(1) \\
&- \frac{5\big(g''(0)\big)^3}{8\sqrt{\pi}}t^{3/2}\theta(3) + O(t^{5/2})
\end{aligned} \tag{4.5}
$$

under the assumption that $y = O(t)$ as $t \to 0$. The next step is to obtain the expansion for the interface after the thresholding step (3.2); at that point, the dependence of the scheme on the convolution kernel K is no longer linear. We substitute the ansatz $y = a_1 t + a_2 t^2 + O(t^3)$ into (4.5) to get

$$K_t * \mathbf{1}_\Sigma(0,y) = A_0 + A_1\sqrt{t} + A_3 t^{3/2} + O(t^{5/2}), \tag{4.6}$$

where

$$A_0 = \frac{1}{2}\theta(0), \tag{4.7}$$

and

$$A_1 = \frac{1}{2\sqrt{\pi}}\Big(\theta(1)g''(0) - a_1\theta(-1)\Big), \tag{4.8}$$

and

$$
\begin{aligned}
A_3 =& \frac{1}{8\sqrt{\pi}}\theta(3)\left(2g^{(\mathrm{iv})}(0) - 5\big(g''(0)\big)^3\right) + \frac{3\big(g''(0)\big)^2}{8\sqrt{\pi}}\theta(1)a_1 \\
&- \frac{g''(0)}{8\sqrt{\pi}}\theta(-1)a_1^2 + \frac{1}{24\sqrt{\pi}}\theta(-3)a_1^3 - \frac{1}{2\sqrt{\pi}}\theta(-1)a_2.
\end{aligned} \tag{4.9}
$$

It turns out that taking $N = 3$ is sufficient for our purposes in this section. Thus, for the rest of this section, we take our kernel K to be of the form

$$K = G + c_1 G_{\alpha_1} + c_2 G_{\alpha_2}. \tag{4.10}$$

From (4.7), we see that the convolution level will be given by

$$\lambda = \frac{1 + c_1 + c_2}{2}. \tag{4.11}$$

Setting (4.6) equal to (4.11), we require $A_1 = 0$ and $A_2 = 0$. At the $O(\sqrt{t})$ level, solving $A_1 = 0$ for a_1, we find

$$a_1 = \frac{\theta(1)}{\theta(-1)} g''(0). \tag{4.12}$$

Having determined a_1, A_3 can now be expressed as

$$\begin{aligned} A_3 =& \frac{\theta(3)}{4\sqrt{\pi}} g^{(\mathrm{iv})}(0) + \frac{\theta^3(1)\theta(-3) + 6\theta^2(1)\theta^2(-1) - 15\theta^3(-1)\theta(3)}{24\sqrt{\pi}\theta^3(-1)} \big(g''(0)\big)^3 \\ &- \frac{\theta(-1)}{2\sqrt{\pi}} a_2. \end{aligned} \tag{4.13}$$

Setting $A_3 = 0$ and solving for a_2, we find

$$a_2 = \frac{\theta(3)}{2\theta(-1)} g^{(\mathrm{iv})}(0) + \frac{\theta^3(1)\theta(-3) + 6\theta^2(1)\theta^2(-1) - 15\theta^3(-1)\theta(3)}{12\theta^4(-1)} \big(g''(0)\big)^3. \tag{4.14}$$

We can now compare (4.12) and (4.14) with (4.2). To match the two expansions for some effective choice of time step size in (3.1) and (3.2), we need

$$\frac{\theta^2(1)}{\theta^2(-1)} = \frac{\theta(3)}{\theta(-1)} \tag{4.15}$$

and

$$\frac{\theta(3)}{\theta(-1)} = -\frac{\theta^3(1)\theta(-3) + 6\theta^2(1)\theta^2(-1) - 15\theta^3(-1)\theta(3)}{12\theta^4(-1)} \tag{4.16}$$

along with the proviso $\theta(-1) \neq 0$ that we will verify at the end. Taking $\alpha_1 = 4$ and $\alpha_2 = 1/4$, (4.15) becomes

$$72c_1 + 18c_2 + 225c_1c_2 = 0, \tag{4.17}$$

which gives

$$c_2 = -\frac{8c_1}{25c_1 + 2}. \tag{4.18}$$

Substituting into (4.16), we get

$$\frac{(10c_1 + 1)^2\big(1000c_1^3 - 2175c_1^2 + 210c_1 + 64\big)}{12(5c_1 + 2)^5} = 0. \tag{4.19}$$

The polynomial

$$p(x) = 1000c_1^3 - 2175c_1^2 + 210c_1 + 64 \tag{4.20}$$

satisfies $p(1/5) = 27$ and $p(1/4) = -61/16$, and hence has a root in $(\frac{1}{5}, \frac{1}{4})$, at which the denominator of (4.19) does not vanish. Taking this root as the value of c_1, i.e.,

$$c_1 \approx 0.2444098, \tag{4.21}$$

(4.19) is then satisfied. Substituting into (4.18) determines c_2:

$$c_2 \approx -0.2410874. \tag{4.22}$$

We note that $\theta(-1) = 1 + \frac{1}{2}c_1 - 2c_2 \neq 0$, as hoped for.

Returning to (4.12), we see that when the convolution kernel F in (3.1) is given by (4.10) with $\alpha_1 = 4$, $\alpha_2 = \frac{1}{4}$, and the two coefficients c_1, c_2 are given by (4.21) and (4.22), and scheme (3.1), (3.2) is *second order accurate* with the (rescaled) effective time step size

$$\tau = \frac{\theta(1)}{\theta(-1)}t = \frac{1 + 2c_1 + \frac{1}{2}c_2}{1 + \frac{1}{2}c_1 + 2c_2}t \approx 2.137831t. \tag{4.23}$$

Figure 1 shows a plot of the radial profile of the kernel. It appears to be positive; we now show that it indeed is.

Let $\xi = \exp(-\frac{1}{16}r^2)$ so that $\xi \in (0, 1]$. Then,

$$K = \frac{1}{\pi}\xi q(\xi), \text{ where } q(\xi) = c_2\xi^{15} + \frac{1}{4}\xi^3 + \frac{1}{16}c_1.$$

We have

$$\begin{aligned} q(\xi) &= \xi^3\left(\frac{1}{4} + c_2\xi^{12}\right) + \frac{1}{16}c_1 \\ &\geq \xi^3\left(\frac{1}{4} + c_2\right) + \frac{1}{16}c_1 \\ &\geq 0 \end{aligned} \tag{4.24}$$

since $c_1 \in (\frac{1}{5}, \frac{1}{4})$, and so $c_2 \in (-\frac{8}{33}, -\frac{8}{35})$. We have established the following claim.

CLAIM 4.1. *Let c_1 be the root of the polynomial* (4.20) *in* $(\frac{1}{5}, \frac{1}{4})$. *Let c_2 be given in terms of c_1 by* (4.18). *Let K be the convolution kernel*

$$K = G + c_2G_4 + c_3G_{\frac{1}{4}}.$$

Then, scheme (3.1), (3.2) *is monotone and second order consistent with curvature motion in the plane. The discrete in time evolutions generated by the scheme (extended from sets to functions in the natural way of, e.g.,* [13]*) converge uniformly to the unique viscosity solution* [10, 4] *of curvature motion on any finite time interval, starting from bounded, uniformly continuous initial data.*

Proof. The claim is an immediate consequence of positivity, smoothness, and decay properties of the kernel, the consistency calculation above, and the theory of [2, 13]. In fact, our kernel satisfies the conditions of [13]. ∎

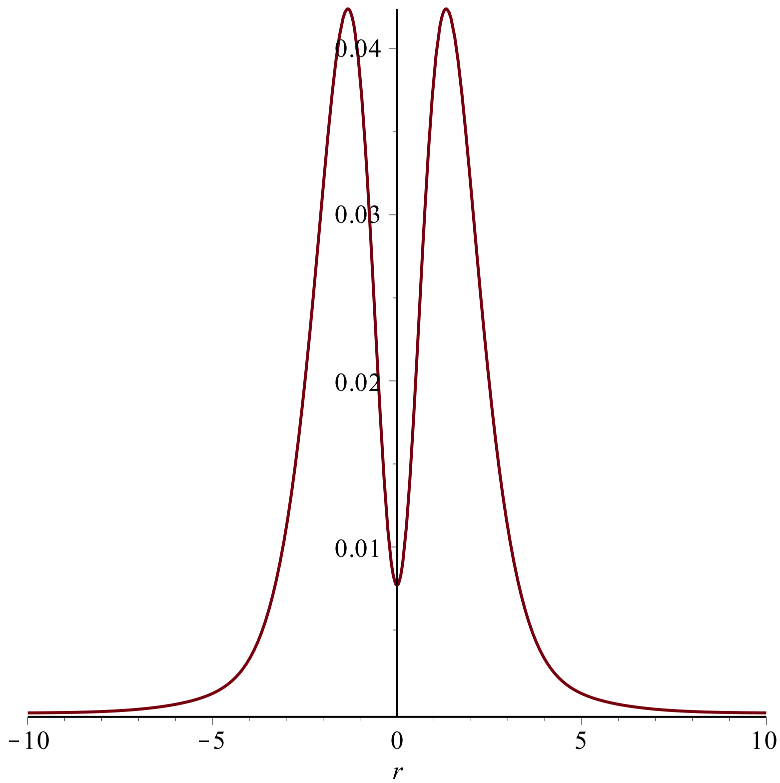

FIG. 1. *Radial profile of the special convolution kernel K that endows the standard threshold dynamics algorithm of Merriman, Bence, and Osher with second order accuracy in two dimensions, as well as with monotonicity.*

5. Numerical demonstration. We demonstrate that second order accuracy (in time) is indeed achieved by scheme (3.1), (3.2) using the convolution kernel (4.10). To that end, and to minimize any potential issues with insufficient spatial resolution, we implement the algorithm 1. in the radial case to test on a shrinking circle, and 2. in case the interface is given as the periodic graph of a function.

For the shrinking circle test, we merely test the local truncation error by taking a single time step (of various sizes) with the algorithm, starting from initial radii of $r_0 = 1, 2$, and 3. In this case, the exact solution of curvature motion is given by $\sqrt{r_0^2 - 2t}$. The convolution in the algorithm is calculated very accurately in polar coordinates. The expected $O(t^3)$ rate of decay of the local error is observed, as shown in Figure 2.

To test on interfaces given as graphs of functions, we measure the global error at final time $T = 1/40$, starting from periodic initial conditions $y = f_0(x)$, where $f_0(x) = \frac{1}{2}\sin(2\pi x)$ and $f_0(x) = \exp(\cos(\pi x))$. The benchmark solution of the PDE (4.1) is obtained by an extremely fine finite differences discretization (forward Euler time steps, and centered differences in space). The algorithm is implemented by discretizing the x-axis, and for each discrete x-value, finding the value of y for which

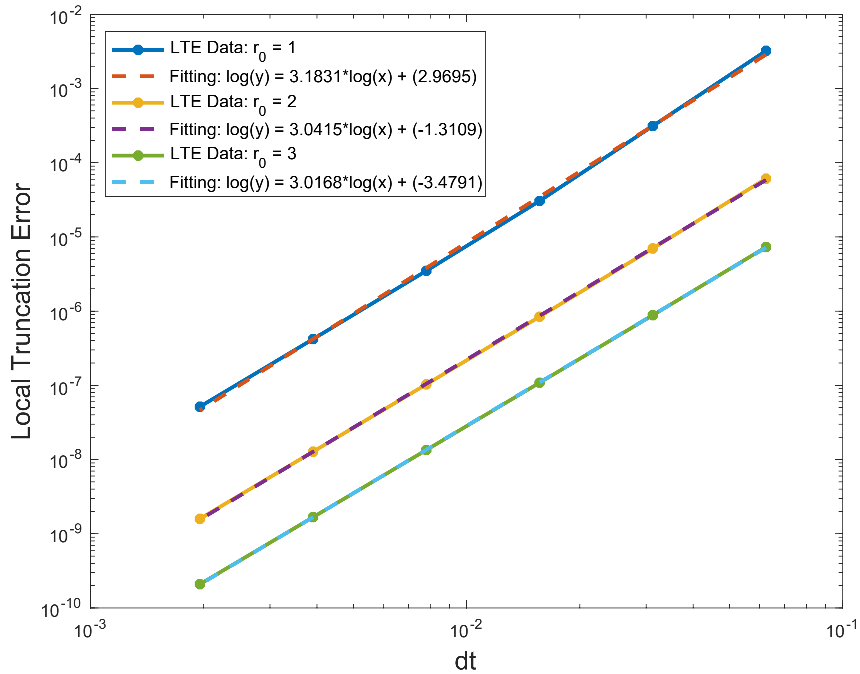

FIG. 2. *Local truncation error for initial condition given by circles of radii* $r_0 = 1, 2, 3$.

the convolution integral

$$
\begin{aligned}
G_t * \mathbf{1}_\Sigma(x,y) &= \int_{-\infty}^{+\infty} G_t(x-\bar{x}) \int_{-\infty}^{f_0(\bar{x})} \frac{1}{\sqrt{4\pi\delta t}} e^{-\frac{(y-\bar{y})^2}{4\delta t}} \, d\bar{y} d\bar{x} \\
&= \frac{1}{2} + \frac{1}{2} \int_{-\infty}^{+\infty} G_t(x-\bar{x}) \operatorname{erf}\left(\frac{f(\bar{x})-y}{2\sqrt{t}}\right) d\bar{x}
\end{aligned} \tag{5.1}
$$

equals the thresholding value λ, where the interface at the current time step is represented by $y = f(x)$. The convolution integral (5.1) is estimated numerically, and its integrand is truncated once it falls below a tolerance. The expected $O(t^2)$ scaling of the global error can be seen in Tables 1 and 2 and Figure 3.

TABLE 1
Error and order for $f_0(x) = \frac{1}{2}\sin(2\pi x)$.

Number of time steps	32	64	128	256	512
L^2 error	3.76e-04	1.04e-04	2.73e-05	6.93e-06	1.70e-06
Order	-	1.9	1.9	2.0	2.0

6. Dimension $d = 3$. In this section, we show that the simple kernel construction of section 4 as a linear combination of Gaussians will not work in higher dimensions. This was mentioned in [25] in passing; here we give a careful explanation. For $d = 3$, assume that the initial interface $\partial\Sigma^0$ is given as the graph of a smooth function $g : \mathbb{R}^2 \to \mathbb{R}$ with $g(0,0) = 0$ and $\nabla g(0,0) = 0$ so that $\Sigma^0 = \{(x,y,z) : z \geq g(x,y)\}$.

TABLE 2
Error and order for $f_0(x) = \exp(\cos(\pi x))$.

Number of time steps	32	64	128	256	512
L^2 error	7.92e-04	2.16e-04	5.67e-05	1.45e-05	3.64e-06
Order	-	1.9	1.9	2.0	2.0

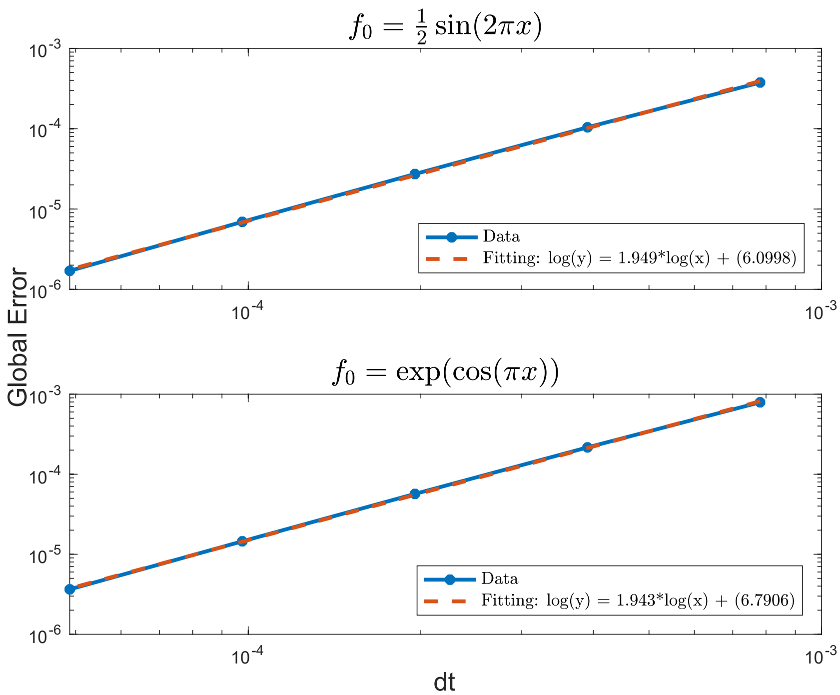

FIG. 3. *Global error for initial condition given $f_0 = \frac{1}{2}\sin(2\pi x)$ and $f_0 = \exp(\cos(\pi x))$.*

The exact solution of motion by mean curvature is described at least for short time by the PDE

$$\begin{cases} \phi_t = \dfrac{(1+\phi_y^2)\phi_{xx} + (1+\phi_x^2)\phi_{yy} - 2\phi_x\phi_y\phi_{x,y}}{1+\phi_x^2+\phi_y^2}, \\ \phi(x,y,0) = g(x,y). \end{cases} \tag{6.1}$$

As in two dimensions, we can obtain a Taylor expansion for the solution at time $t > 0$:

$$\begin{aligned} \phi(0,0,t) &= tH(0,0) + \frac{1}{2}t^2\left\{\Delta^2 g(0,0) - 2H^3(0,0) + 6H(0,0)\kappa(0,0)\right\} + O(t^3) \\ &= tH(0,0) + \frac{1}{2}t^2\left\{\Delta_S H(0,0) + H^3(0,0) - 2H(0,0)\kappa(0,0)\right\} + O(t^3), \end{aligned} \tag{6.2}$$

where

$$\begin{aligned} H(0,0) &= \Delta g(0,0) = g_{xx}(0,0) + g_{yy}(0,0), \\ \kappa(0,0) &= g_{xx}(0,0)g_{yy}(0,0) - g_{xy}^2(0,0), \\ \Delta_S H(0,0) &= \Delta^2 g(0,0) - 3H^3(0,0) + 8H(0,0)\kappa(0,0). \end{aligned} \tag{6.3}$$

Taylor expansion for the convolution step (3.1) using the standard Gaussian kernel has also been obtained in higher dimensions $d \geq 3$ in multiple previous studies; combining, for instance, formula (3.3) in [25] for $d = 3$ with (6.3), we get

$$
\begin{aligned}
G_t * \mathbf{1}_{\Sigma^0}(0,0,z) =& \frac{1}{2} - \frac{1}{2\sqrt{\pi}}\frac{z}{\sqrt{t}} + \frac{1}{24\sqrt{\pi}}\frac{z^3}{t^{3/2}} + \frac{H(0,0)}{2\sqrt{\pi}}\sqrt{t} \\
&+ \frac{\Delta^2 g(0,0)}{4\sqrt{\pi}}t^{3/2} - \frac{1}{8\sqrt{\pi}}\frac{z^2}{\sqrt{t}}H(0,0) \\
&+ \frac{1}{2\sqrt{\pi}}z\sqrt{t}\left(\frac{3}{4}H^2(0,0) - \kappa(0,0)\right) \\
&- \frac{1}{2\sqrt{\pi}}t^{3/2}\left(\frac{5}{4}H^3(0,0) - 3H(0,0)\kappa(0,0)\right) + O(t^{5/2}).
\end{aligned} \tag{6.4}
$$

Then the Taylor expansion for the convolution step (3.1) of scheme (3.1), (3.2) using a linear combination of Gaussian kernels is now given by

$$
\begin{aligned}
K_t * \mathbf{1}_{\Sigma^0}(0,0,z) =& \frac{1}{2}\theta(0) - \frac{1}{2\sqrt{\pi}}\frac{z}{\sqrt{t}}\theta(-1) + \frac{1}{24\sqrt{\pi}}\frac{z^3}{t^{3/2}}\theta(-3) + \frac{H(0,0)}{2\sqrt{\pi}}\sqrt{t}\theta(1) \\
&+ \frac{\Delta^2 g(0,0)}{4\sqrt{\pi}}t^{3/2}\theta(3) - \frac{1}{8\sqrt{\pi}}\frac{z^2}{\sqrt{t}}H(0,0)\theta(-1) \\
&+ \frac{1}{2\sqrt{\pi}}z\sqrt{t}\left(\frac{3}{4}H^2(0,0) - \kappa(0,0)\right)\theta(1) \\
&- \frac{1}{2\sqrt{\pi}}t^{3/2}\left(\frac{5}{4}H^3(0,0) - 3H(0,0)\kappa(0,0)\right)\theta(3) + O(t^{5/2}).
\end{aligned} \tag{6.5}
$$

Substituting the ansatz $z = a_1 t + a_2 t^2 + O(t^3)$, we get

$$K_t * \mathbf{1}_{\Sigma^0}(0,0,z) = A_0 + A_1\sqrt{t} + A_3 t^{3/2} + O(t^{5/2}), \tag{6.6}$$

where

$$A_0 = \frac{\theta(0)}{2}, \tag{6.7}$$

and

$$A_1 = \frac{1}{2\pi}\Big(\theta(1)H(0,0) - a_1\theta(-1)\Big), \tag{6.8}$$

and

$$
\begin{aligned}
A_3 =& -\frac{\theta(-1)}{2\sqrt{\pi}}a_2 + \frac{\theta(-3)}{24\sqrt{\pi}}a_1^3 + \frac{\theta(3)}{4\sqrt{\pi}}\Delta^2 g(0,0) - \frac{\theta(-1)}{8\sqrt{\pi}}a_1^2 H(0,0) \\
&+ \frac{\theta(1)}{2\sqrt{\pi}}a_1\left(\frac{3}{4}H^2(0,0) - \kappa(0,0)\right) - \frac{\theta(3)}{2\sqrt{\pi}}\left(\frac{5}{4}H^3(0,0) - 3H(0,0)\kappa(0,0)\right).
\end{aligned} \tag{6.9}
$$

Choosing the thresholding level as

$$\lambda = \frac{\theta(0)}{2} = \frac{1}{2}\sum_{j=1}^{N} c_j, \tag{6.10}$$

we set $A_1 = 0$ and solve for a_1 to obtain

$$a_1 = \frac{\theta(1)}{\theta(-1)} H(0,0). \tag{6.11}$$

Having determined a_1, we substitute the expression for it into A_3 and solve for a_2 to obtain

$$\begin{aligned} a_2 =& \frac{\theta(3)}{2\theta(-1)} \Delta^2 g(0,0) \\ &+ \frac{\theta^3(1)\theta(-3) + 6\theta^2(1)\theta^2(-1) - 15\theta(3)\theta^3(-1)}{12\theta^4(-1)} H^3(0,0) \\ &- \frac{\theta^2(1) - 3\theta(3)\theta(-1)}{\theta^2(-1)} H(0,0)\kappa(0,0). \end{aligned} \tag{6.12}$$

Thus, in summary, the location of the interface along the z-axis after one time step with scheme (3.1), (3.2) is given by

$$z = tB_1 H(0,0) + t^2 \left\{ B_2 \Delta^2 g(0,0) + B_3 H^3(0,0) + B_4 H(0,0)\kappa(0,0) \right\}, \tag{6.13}$$

where

$$\begin{aligned} B_1 &= \frac{\theta(1)}{\theta(-1)}, \\ B_2 &= \frac{\theta(3)}{2\theta(-1)}, \\ B_3 &= +\frac{\theta^3(1)\theta(-3) + 6\theta^2(1)\theta^2(-1) - 15\theta(3)\theta^3(-1)}{12\theta^4(-1)}, \text{ and} \\ B_4 &= -\frac{\theta^2(1) - 3\theta(3)\theta(-1)}{\theta^2(-1)}. \end{aligned} \tag{6.14}$$

To match the exact expansion (6.2) for some possibly rescaled effective time step size, we need, in particular,

$$6B_2 = B_4, \tag{6.15}$$

which, under the proviso that $\theta(-1) \neq 0$, implies $B_1 = 0$. That precludes matching (6.2) up to $O(t^3)$ terms. Hence, second order consistency with motion by mean curvature cannot be obtained using any linear combination of Gaussians as the convolution kernel in dimensions $d \geq 3$, even at the expense of violating the comparison principle (i.e., allowing the kernel to become negative). In particular, the special linear combination of Gaussians exhibited in section 4 that attains second order accuracy on curves in $\mathbb{R}^2$ degrades to first order accuracy for a general surface in $\mathbb{R}^3$. The leading order error term entails the product $H(0,0)\kappa(0,0)$ of the mean and Gaussian curvatures of the surface.

7. Conclusion. We have exhibited a second order accurate in time scheme for curvature motion in the plane that is monotone: It preserves the comparison principle satisfied by the exact evolution it approximates. The scheme is a variant of the threshold dynamics algorithm of Merriman, Bence, and Osher. In particular, we have shown that there is a very special convolution kernel—a carefully chosen linear combination of Gaussians—to use in that algorithm that endows the scheme with both second order accuracy in time and monotonicity. Numerical experiments presented bear out the advertised order of accuracy. We have also shown that extending our work to three dimensions and higher will require a convolution kernel that cannot be as simple as a linear combination of Gaussians. Some immediate, intriguing directions for further study include the following:

- Is there a more elaborate kernel construction that would result in a monotone, second order accurate algorithm of the form (3.1), (3.2) in three dimensions and higher?
- The two dimensional special convolution kernel identified in section 4 is positive (which is what makes the resulting algorithm monotone), but its Fourier transform isn't. This means the resulting scheme is not guaranteed to dissipate the Lyapunov functional identified in [7]. Is there another kernel that results in second order accuracy in time, and that is positive in both physical and Fourier domains, so that both the comparison principle and energy based notions of stability are guaranteed?
- We already know that the scheme is convergent to the viscosity solution of curvature motion, thanks to consistency and monotonicity. Given that consistency holds at second order, can the rate of convergence be rigorously shown to be second order in time, as in [14], which establishes first order convergence for the original algorithm?
- Are there related geometric motions for which a similar thresholding scheme can be found that is monotone and second order?

REFERENCES

[1] G. Barles and C. Georgelin, *A simple proof of convergence for an approximation scheme for computing motions by mean curvature*, SIAM J. Numer. Anal., 32 (1995), pp. 484–500, https://doi.org/10.1137/0732020.

[2] G. Barles and P. Souganidis, *Convergence of approximation schemes for fully nonlinear second order equations*, Asymptot. Anal., 4 (1991), pp. 271–283.

[3] E. Bonnetier, E. Bretin, and A. Chambolle, *Consistency result for a non-monotone scheme for anisotropic mean curvature flow*, Interfaces Free Bound., 14 (2012), pp. 1–35.

[4] Y.-G. Chen, Y. Giga, and S. Goto, *Uniqueness and existence of viscosity solutions of generalized mean curvature flow equations*, J. Differential Geom., 33 (1991), pp. 749–786.

[5] M. Elsey and S. Esedoḡlu, *Threshold dynamics for anisotropic surface energies*, Math. Comp., 87 (2018), pp. 1721–1756.

[6] S. Esedoḡlu, M. Jacobs, and P. Zhang, *Kernels with prescribed surface tension & mobilty for threshold dynamics schemes*, J. Comput. Phys., 337 (2017), pp. 62–83.

[7] S. Esedoḡlu and F. Otto, *Threshold dynamics for networks with arbitrary surface tensions*, Comm. Pure Appl. Math., 68 (2015), pp. 808–864.

[8] S. Esedoḡlu, S. Ruuth, and Y.-H. Tsai, *Threshold dynamics for high order geometric motions*, Interfaces Free Bound., 10 (2008), pp. 263–282.

[9] L. C. Evans, *Convergence of an algorithm for mean curvature motion*, Indiana Univ. Math. J., 42 (1993), pp. 553–557.

[10] L. C. Evans and J. Spruck, *Motion of level sets by mean curvature.* I, J. Differential Geom., 33 (1991), pp. 635–681.

[11] R. Grzhibovskis and A. Heintz, *A convolution-thresholding approximation of generalized curvature flows*, SIAM J. Numer. Anal., 42 (2005), pp. 2652–2670, https://doi.org/10.1137/S0036142903431316.

[12] R. Grzhibovskis and A. Heintz, *A convolution thresholding scheme for the Willmore flow*, Interfaces Free Bound., 10 (2008), pp. 139–153.

[13] H. Ishii, G. E. Pires, and P. E. Souganidis, *Threshold dynamics type approximation schemes for propagating fronts*, J. Math. Soc. Japan, 51 (1999), pp. 267–308.

[14] K. Ishii, *Optimal rate of convergence of the Bence–Merriman–Osher algorithm for motion by mean curvature*, SIAM J. Numer. Anal., 37 (2005), pp. 841–866, https://doi.org/10.1137/

04061862X.
[15] T. Laux and F. Otto, *Convergence of the thresholding scheme for multi-phase mean-curvature flow*, Calc. Var. Partial Differential Equations, 55 (2016), 129.
[16] T. Laux and F. Otto, *Brakke's inequality for the thresholding scheme*, Calc. Var. Partial Differential Equations, 59 (2020), pp. 39–65.
[17] P. Mascarenhas, *Diffusion Generated Motion by Mean Curvature*, CAM Report 92-33, UCLA, 1992.
[18] B. Merriman, J. K. Bence, and S. Osher, *Motion of multiple junctions: A level set approach*, J. Comput. Phys., 112 (1994), pp. 334–363.
[19] B. Merriman, J. K. Bence, and S. J. Osher, *Diffusion generated motion by mean curvature*, in Proceedings of the Computational Crystal Growers Workshop, J. Taylor, ed., AMS, 1992, pp. 73–83.
[20] S. Ruuth, *Efficient Algorithms for Diffusion-generated Motion by Mean Curvature*, Ph.D. thesis, University of British Columbia, Vancouver, 1996.
[21] S. J. Ruuth, *Efficient algorithms for diffusion-generated motion by mean curvature*, J. Comput. Phys., 144 (1998), pp. 603–625.
[22] S. J. Ruuth and B. Merriman, *Convolution generated motion and generalized Huygens' principles for interface motion*, SIAM J. Appl. Math., 60 (2000), pp. 868–890, https://doi.org/10.1137/S003613999833397X.
[23] D. Swartz and N. K. Yip, *Convergence of diffusion generated motion to motion by mean curvature*, Comm. Partial Differential Equations, 42 (2017), pp. 1598–1643.
[24] N. Walkington, *Algorithms for computing motion by mean curvature*, SIAM J. Numer. Anal., 33 (1996), pp. 2215–2238, https://doi.org/10.1137/S0036142994262068.
[25] A. Zaitzeff, S. Esedoḡlu, and K. Garikipati, *Second order threshold dynamics schemes for two phase motion by mean curvature*, J. Comput. Phys., 410 (2020), 109404.